Implications of regional surface ozone increases on visibility degradation in southeast China

Mang Lin, Iat-Neng Chan, Chuen-Yu Chan, Guenter Engling & William Bloss

Implications of regional surface ozone increases on visibility degradation in southeast China

By MANG LIN[1], IAT-NENG CHAN[2], CHUEN-YU CHAN[3]*, GUENTER ENGLING[4] and WILLIAM BLOSS[5], *[1]School of Environmental Science and Engineering, Sun Yat-sen University, Guangzhou, China; [2]Faculty of Science and Technology, University of Macao, Macao, China; [3]Faculty of Science and Engineering, University of Nottingham Ningbo China, Ningbo, China; [4]Department of Biomedical Engineering and Environmental Sciences, National Tsing Hua University, Hsinchu, Taiwan; [5]School of Geography, Earth and Environmental Sciences, University of Birmingham, Birmingham B15 2TT, UK*

ABSTRACT

Long-term visibility (1968–2010) and air pollutant (1984–2010) data records in Hong Kong reveal that the occurrence of reduced visibility (RV, defined as the percentage of hours per month with visibility below 8 km in the absence of rain, fog, mist or relative humidity above 95%) in southeast China has increased significantly in the last four decades. The most pronounced rate of increase was observed after 1990 (nine times higher than that before 1990), when notable increases in surface ozone (O_3) levels were simultaneously observed ($1.06 \ \mu g \ m^{-3}$ per yr). The greatest increases in RV, and in O_3, NO_2 and SO_2 concentrations are coincident in the autumn (1.47, 0.20 and $0.45 \ \mu g \ m^{-3}$ per yr respectively), when southeast China is strongly influenced by regional O_3 formation and accumulation due to continental outflow of pollution from the east China coast under favourable meteorological conditions. Multiple regression revealed that the RV percentage correlated well ($p < 0.05$) with NO_2 and NO_x in the 1980s, and with NO_2, SO_2 and O_3 after the 1990s, suggesting that there have been changes in the predominant factors causing visibility degradation. In order to elucidate the reasons for these changes, the results were integrated with data from previous research. Possible impacts of elevated O_3 on secondary particle formation and their effects on visibility degradation and aerosol radiative forcing in an oxidant-enhanced southeast China are highlighted. Other factors potentially leading to visibility degradation, such as ship emissions and biomass burning, are also discussed.

Keywords: visibility, surface ozone, secondary particle, atmospheric oxidation capacity

1. Introduction

The severe air pollution manifested by frequent occurrence of hazy days in China and its impact on the ecosystem and regional climate have been a major concern of the general public and a focus of the international scientific community in recent years (e.g., Shao et al., 2006; Rosenfeld et al., 2007; Thach et al., 2010). Satellite remote sensing and ground-based measurements have revealed that there have been significant increases of air contaminants in the atmosphere over China (e.g., Chan et al., 2004; Richter et al., 2005; Lin et al., 2010a). Visibility data recorded across China also revealed that visibility across the country has been degrading rapidly, especially in the urban and industrial centres, such as the Pearl River Delta (PRD), Yangtze River Delta, and Beijing in eastern China, due to the escalating air pollution associated with increasing fossil fuel combustion and industrial development (Che et al., 2007; 2009).

The PRD is one of the regions with the most dramatic visibility degradation in China. Long-term visibility trends in this region and their causes have been examined over the past decade. In Guangzhou, the capital city of the PRD, severe visibility degradation has been observed frequently since 1954, and recent field observations with chemical speciation of the aerosol suggested that fine particles, especially elemental carbon (EC), play an important role in this visibility reduction (Deng et al., 2008). Visibility reduction was recently found to occur for 22% of the time over the period from 1998 to 2008 in Foshan, an industrial city in the PRD, again related to (significantly correlated with)

---

*Corresponding author.
email: John.Chan@nottingham.edu.cn

1

concentrations of particulate matter (Wan et al., 2011). In Hong Kong, a noticeable reduction in visibility has also been noted based on earlier records (Leung et al., 2004; Thach et al., 2010). Wang (2003) showed that fine particulates, with aerodynamic diameters of 2.5 μm and less ($PM_{2.5}$), especially associated with ammonium sulphate, are the largest contributor to visibility degradation during episodic poor visibility events.

The visibility record has been found to have a vital implication for public health research owing to the contribution of fine particulates (Huang et al., 2009; Thach et al., 2010), and to regional climate due to aerosol radiative forcing (Rosenfeld et al., 2007). Therefore, it is imperative to understand the relationship between visibility degradation and air quality deterioration, and the underlying physical and chemical mechanisms. Located in the southeastern part of the country at the edge of the PRD region, Hong Kong is strongly impacted by air pollutants transported from upwind source regions along the east Asian coast, particularly under the influence of the winter monsoon. With continuous urban and industrial development in eastern and southern China, including the PRD, it is important to explore the long-term changes in pollutant levels resulting from such development, and their effect on visibility in Hong Kong. Fortunately, visibility in Hong Kong has been continuously monitored by the Hong Kong Observatory (HKO) since the late 1960s, and principal air quality parameters have been measured by the Hong Kong Environmental Protection Department (HKEPD) starting in the early 1980s, coincident with the establishment of the open-door policy of China in the late 1970s. Subject to strict quality assurance (QA) and quality control (QC) procedures during monitoring and data processing (Chan et al., 2004), these high quality datasets represent one of the longest records in China, allowing for the assessment of long-term changes in air quality in southeast China and the PRD. For instance, Chan et al. (2004) derived the first 'background' ozone trends from the urban data records, which were subsequently confirmed by measurements at a rural site (Wang et al., 2009).

In this paper, we examine 43-yr visibility and 27-yr air quality datasets from Hong Kong in order to characterise their long-term trends and statistical relationships, and to ascertain their implications for atmospheric chemistry in southeast China. We first consider the seasonal cycles, overall trends and trends across the four seasons of visibility and air quality. Secondly, a multiple linear regression method is applied to investigate the underlying relationships between air quality and visibility. Finally, the enhanced oxidizing power in the atmosphere of southeast China and its possible effects on visibility degradation is highlighted. The likely dominant chemical mechanisms, leading to formation of secondary particulate matter (especially sulphate) in such an oxidant-rich atmosphere are discussed.

2. Data and methods

2.1. Description of observation sites and datasets

Atmospheric visibility data covering the period from January 1968 to December 2010 were provided by the HKO. The visibility was recorded by experienced observers every hour at the headquarters of the HKO, located in the urban centre of Hong Kong at Tsim Sha Tsui on the Kowloon Peninsula (Fig. 1), according to the standard method set by the HKO (HKO, www.weather.gov.hk). Meteorological data, including precipitation and relative humidity, were also recorded at the headquarters of HKO, while wind direction data were observed at an outlying island located in southeast Hong Kong (Waglan Island, Fig. 1). The visibility data are reported here as monthly Reduced Visibility (RV) in form of the percentage of hours within each month with visibility below 8 km, excluding cases of visibility impairment that were concurrent with precipitation, fog, mist or relative humidity above 95% based on the definition of the HKO (Leung et al., 2004). Under this definition, the resulting low visibility data (RV percentage) are believed to be an accurate indicator of the visibility degradation due to elevated atmospheric pollutant levels. Because the precipitation frequency in the Hong Kong region does not show any significant trend over the time period considered here (Liu et al., 2010), we believe it does not exert any significant impact on the derived long-term RV trends. Changes in mixing layer height may also influence visibility (Sequeira and Lai, 1998; Tsai, 2005), but the different trends of different air pollutants (shown in Section 3) suggested that it is not the major cause of the visibility trends.

Ambient SO_2, PM_{10}, NO_x, NO_2 and O_3 data were obtained from an automatic air quality monitoring station operated by HKEPD situated in a residential area built along the slope of a hill (at an altitude of 78 m above sea level), which is ∼4 km from the visibility observation station (Central/Western, Fig. 1). This station was selected because the available data covered the longest measurement period (starting in 1984) and there have been relatively few changes in the neighbourhood surrounding the station compared with many other stations of Hong Kong. This allows the data to better reflect the general situation of the Hong Kong region rather than the local surroundings of the station itself (Chan et al., 2004). Additionally, this Central/Western station is located at the side of Victoria Harbour (while HKO is situated at the other side, Fig. 1). Due to the complex geographical barrier on both sides of this harbour, the prevailing wind at this location will

Fig. 1. Locations of the Hong Kong Observatory, Air Quality Monitoring Station (Central/Western) and Waglan Island.

be easterly (Channel effect, Fig. 1), and hence will carry the majority of very local traffic emissions away from the monitoring station (Yeung et al., 1990; Chan et al., 2004), reducing the influence of local emissions at the air quality station, and rendering the data from this site to better reflect regional air pollution conditions (Chan and Chan, 2000).

Measurements of O_3 and SO_2 were made by UV absorption (TECO 49) and fluorescence analyzers (TECO 43A), respectively. NO_x was detected by a chemiluminescent analyzer (TECO 42) by continuous measurement of NO and NO_2, while PM_{10} was measured by a tapered element oscillating microbalance (TEOM). The measurement methods have been constant throughout the time period considered here, with the exception of O_3 measurement using a Dasibi 1003-RS UV light analyzer in the early days

(regularly calibrated by a TECO Model 49 O_3 calibrator). Detailed descriptions of these methods can be found in the literature (e.g., Chan et al., 2004; HKEPD, 2010; Thach et al., 2010). The gaseous pollutant data used in this study covered the period from January 1984 to December 2010. However, PM_{10} measurement at this station began in 1993 and thus the PM_{10} data only cover the period from January 1993 to December 2010. The hourly data provided by HKEPD have been subject to strict QA/QC procedures, similar to those required by the Environmental Protection Agency of the United States, which have again been kept consistent throughout the period considered (HKEPD, www.epd.gov.hk). A threshold of minimum hourly data capture rate of 67% was applied to determine the valid monthly and yearly average data.

2.2. Trend and correlation analysis by regression

Long-term trends of visibility and air pollutants were quantified using a simple linear regression model in which annual means (or annual seasonal mean) were the dependent variables. The results were tested with a student t-test to examine the significance of the slope of the resulting regression equations, which was considered as the magnitude of its long-term trend with respect to time. The relationships between monthly RV and concentrations of pollutants were examined using a multiple regression and partial correlation technique. The regression results were subjected to an F test for determination of the statistical significance levels of the resulting regression equations (i.e., the coefficient of determination, R^2) describing the best fitted line for the dependent variables (i.e., RV) and the corresponding independent variables (i.e., pollutant concentrations). In addition, a t-test was applied to examine the significance of the regression coefficients and partial correlation coefficients of the individual independent variables. The statistical significance level of both f-test and t-test were set at 0.05. The partial correlation approach eliminates mutual interactions between independent variables, which simultaneously exist between RV and pollutant concentrations.

3. Results and discussions

3.1. Long-term trends of visibility from 1968 to 2010

With an average growth rate of 0.31% per yr (Table 1), the occurrence of RV in Hong Kong increased from 1.8% in 1968 to a maximum of 17.9% in 2004, followed by a decrease to 14.0% in 2010 (Fig. 2). As shown by Fig. 2, the annual increase rate of the RV percentage was particularly high after 1990, at 0.61% per yr nine times higher than that over the period from 1968 to 1990. These findings suggest that the visibility and hence air quality degradation were more pronounced after 1990, when visibility in other parts of China also started to decrease significantly (e.g., Fig. 2a in Che et al., 2007). Table 1 shows the trends in RV between annual seasonal means in each of four seasons (winter: December–February; spring: March–May; summer: June–August; autumn: September–November), to illustrate the inter-annual changes between the different seasons (Table 1). The increase rates in winter (0.48% per yr from 1968 to 2008, and 0.80% per yr from 1990 to 2008) and autumn (0.43% per yr from 1968 to 2008, and 0.90% per yr from 1990 to 2008) are noticeably higher than those in spring and summer – a significant trend in summer is not apparent. To understand this behaviour, a detailed understanding of causes of this seasonal pattern is needed.

The clear seasonal pattern with a maximum in winter and a minimum in summer (Fig. 3) is in good agreement with Qin and Yang's (2000) findings, which showed the lowest visibility occurring in winter (the heating period) in northern China due to the high coal usage and associated aerosol emissions. Although commercial (not including power plants) and domestic coal usage in southeast China is less extensive compared with that in northern China, the prevalent northeasterly winds in the dry season (from mid-September to mid-April, Figs. 3, 4) facilitate pollutant transport from east Asia, including the coastal areas of mainland China, to the southern part of the country, resulting in substantial pollution episodes in Hong Kong during this season (Chan and Chan, 2000). Other contributing factors to this pattern may be the higher summer

Table 1. Overall and seasonal annual trends of RV, SO_2, NO_2, NO_x, O_3, and PM_{10} (winter: December, January, and February; spring: March, April, and May; summer: June, July, and August; autumn: September, October, and November)

	Period	Overall	Winter	Spring	Summer	Autumn
Reduced visibility (% per yr)	1968–2008	0.31% (p < 0.001)	0.48% (p < 0.001)	0.22% (p < 0.001)	0.11% (p < 0.001)	0.43% (p < 0.001)
	1990–2008	0.61% (p < 0.001)	0.80% (p < 0.001)	0.58% (p < 0.001)	No trend[a]	0.90% (p < 0.001)
O_3 (µg m^{-3} per yr)	1984–2008	0.90 (p < 0.001)	0.75 (p < 0.001)	0.98 (p < 0.001)	0.63 (p < 0.001)	1.47 (p < 0.001)
	1990–2008	1.06 (p < 0.001)	1.06 (p < 0.001)	1.20 (p < 0.001)	0.76 (p < 0.001)	1.32 (p < 0.001)
SO_2 (µg m^{-3} per yr)	1984–2008	No trend	No trend	No trend	No trend	0.20 (p < 0.01)
NO_2 (µg m^{-3} per yr)	1984–2008	No trend	No trend	No trend	No trend	0.45 (p < 0.10)
NO_x (µg m^{-3} per yr)	1984–2008	No trend	No trend	No trend	No trend	No trend
PM_{10} (µg m^{-3} per yr)	1993–2008	No trend	No trend	No trend	No trend	No trend

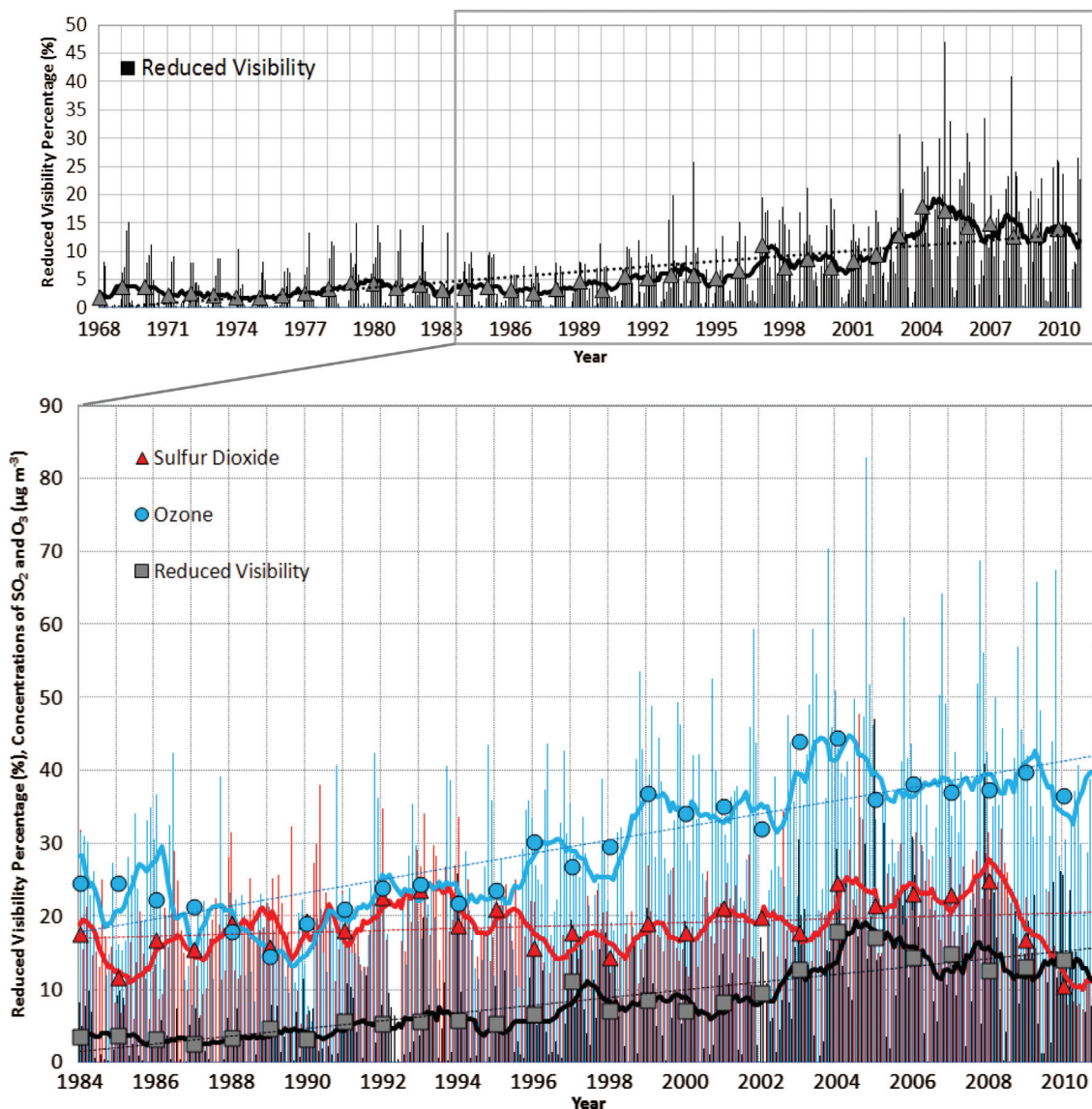[a]'No Trend' indicates that the trend is statistically insignificant at the significance level of 0.10.

Fig. 2. Time series of RV occurrence, concentrations of SO_2 and O_3. (Bars, symbols, solid lines and dotted lines show monthly mean, annual mean, 12-month running mean and overall linear regression trend, respectively.)

rainfall abundance, leading to pollutant washout (Fig. 3) and higher mixing layer height (i.e., better dispersion capacity of the atmosphere) during summer due to solar thermal heating (Sequeira and Lai, 1998).

This pollutant transport mechanism is supported by the high numbers of moderately hazy days and hazy days (defined as days with 1–12 and 13–24 h (respectively) with visibility below 8 km, excluding cases of visibility impairment that were concurrent with precipitation, fog, mist or relative humidity above 95%), which were accompanied by the prevailing northeasterly winds (Fig. 4). The 120-h backward air mass trajectories arriving at 14:00 local time on each moderately hazy day and hazy day calculated via the Hybrid Single Particle Lagrangian Integrated

Trajectory Model (HYSPLIT) (Draxler and Rolph, 2010; Rolph, 2010) also show that on hazy days during winter, most of the air masses originated from the northeast direction (Fig. 5). It is interesting to note that there were also a number of moderately hazy days with prevalent south-westerly winds in summer (Figs. 4, 5), with the majority of air masses originating in the upwind South China Sea. The cause for this type of visibility degradation events is unclear. Cases of long-range transport of levoglucosan, a chemical tracer of biomass burning smoke, have been identified in maritime air masses tracing back to the biomass burning region over the Philippines (Sang et al., 2011; Zhang et al., 2011). The possible impact of this type of smoke aerosol to visibility impairment remains
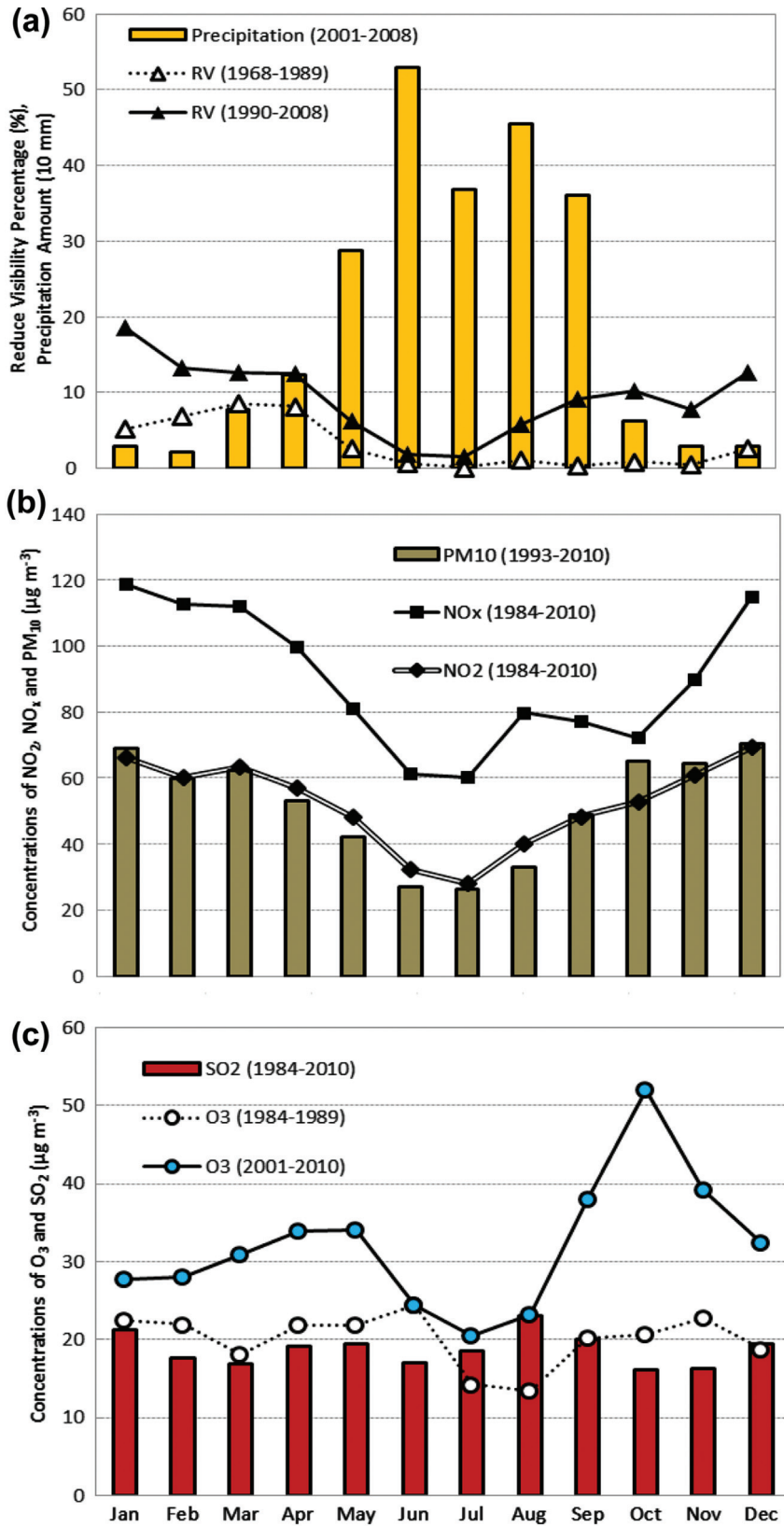
Fig. 3.   Seasonal Patterns of (a) precipitation and RV, (b) concentrations of PM$_{10}$, NO$_2$, NO$_x$, (c) SO$_2$, and O$_3$.
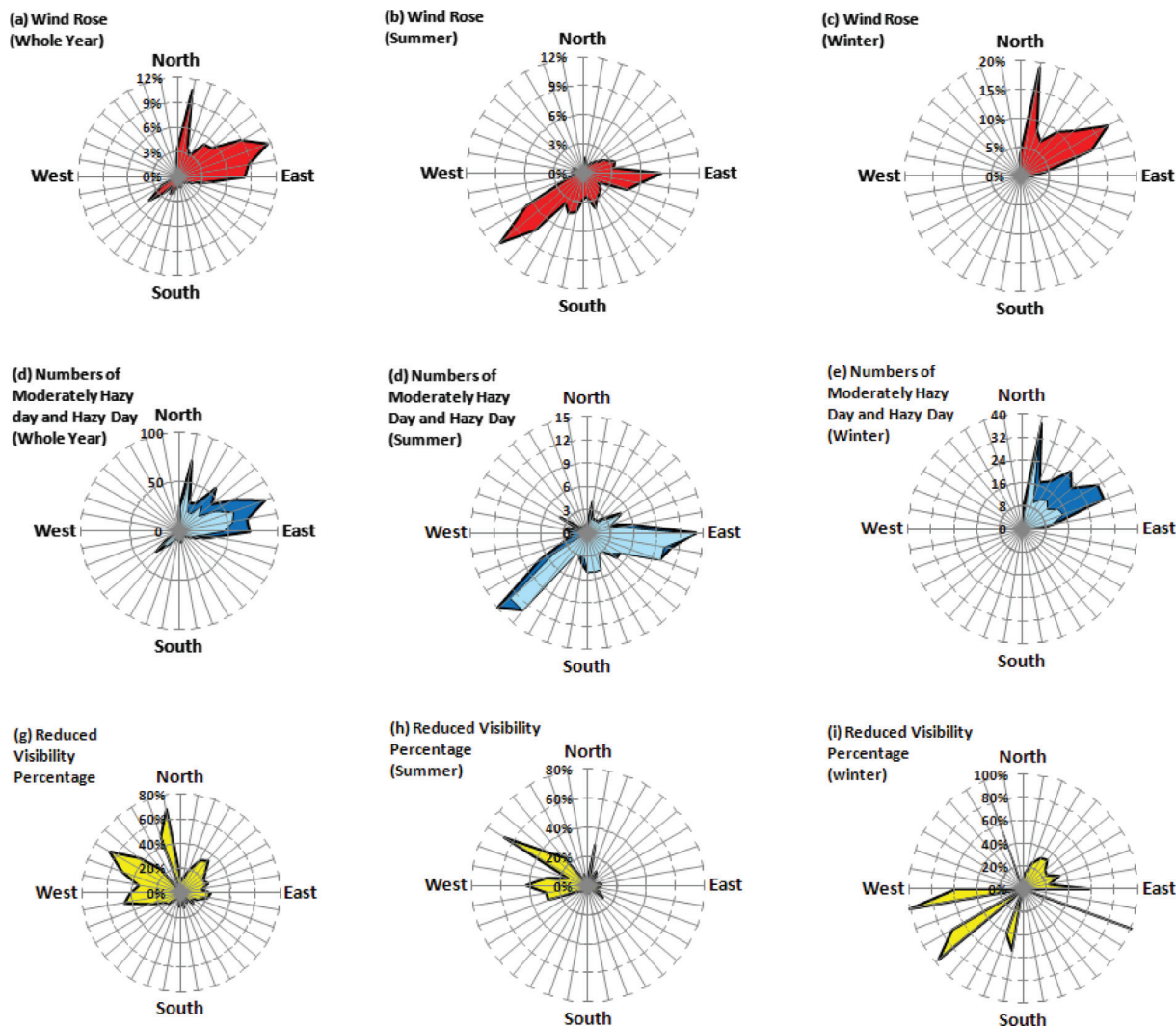
Fig. 4. (a, b, c) Wind roses, (d, e, f) number of moderately hazy days (light blue) and hazy days (blue) and (g, h, i) RV vs. wind direction sectors during 2001–2004.

elusive and thus deserves further study. As Hong Kong is directly affected by emissions in the PRD region when northwesterly winds are prevailing, occurrence of RV during northwesterly wind sectors was found to be higher than that in northeasterly wind sectors. However, such cases are very rare (Figs. 4 and 5), and typically only occur when Hong Kong is influenced by tropical cyclones (Chan and Chan, 2000; Zhang et al., 2010).

The most prominent long-term changes in autumn and winter as illustrated above (Table 1, Fig. 3) might suggest that the increasing RV in Hong Kong during recent years is mainly due to the rapid development in the upwind region, i.e., the highly populated cities in eastern China, which have also suffered from serious visibility degradation (Che et al., 2007; 2009). Correspondingly, the dearth of significant trends in summer suggested that the impact of

local emissions on the observed long-term visibility degradation is relatively small.

3.2. Changes of surface ozone levels and related species during 1984–2010

The seasonal variation of air pollutants, with the exceptions of O_3 and SO_2, were similar to those of RV (Fig. 3), indicating the inherent relationship between air pollution and visibility degradation. These seasonal patterns are driven primarily by the continental monsoon in winter and maritime monsoon in summer. More detailed discussions on these seasonal patterns can be found in the literature (e.g., Chan et al., 1998; Lam et al., 2001; Wan et al., 2011). Ozone concentrations showed a noticeable peak in autumn and a secondary peak in spring, while
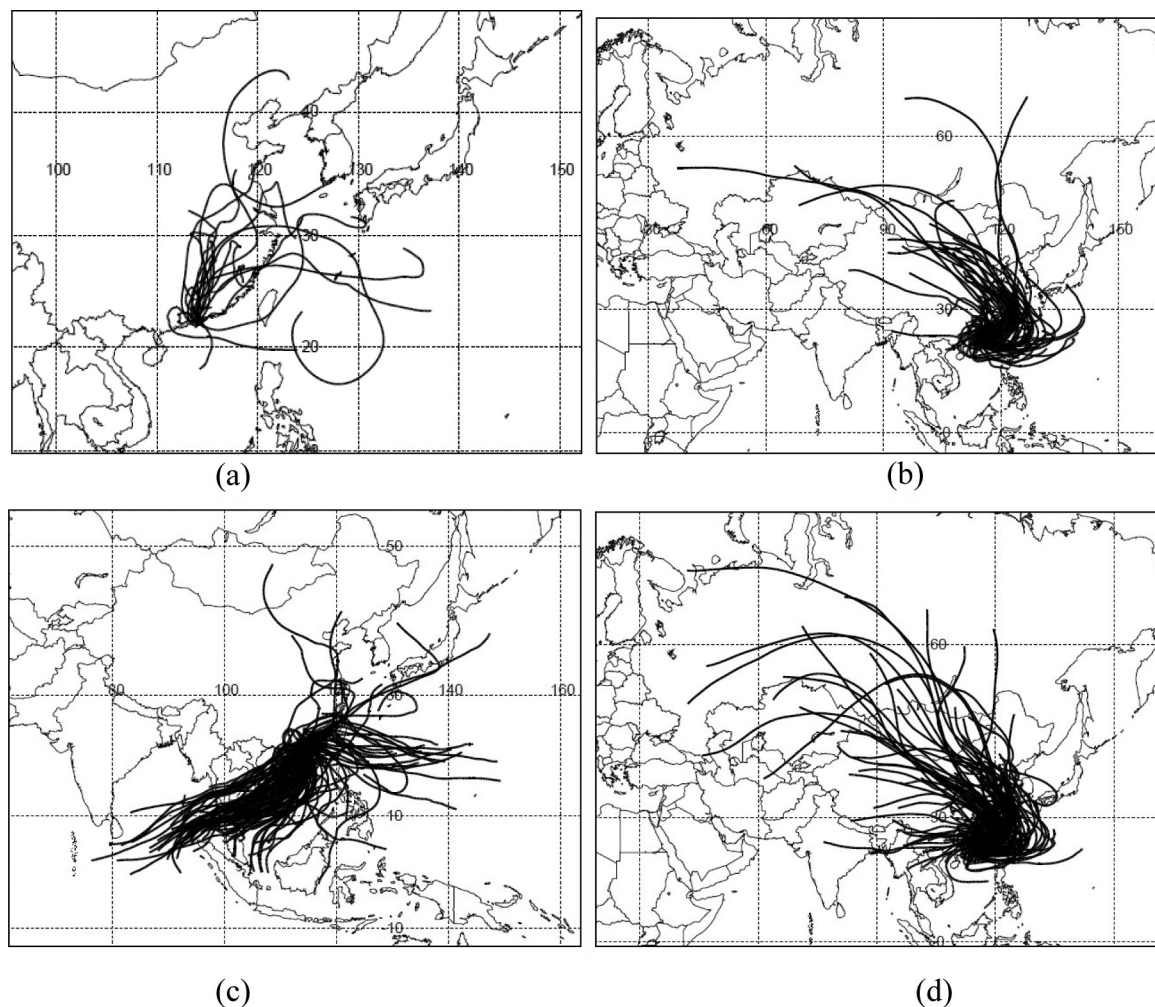
Fig. 5. 120-h backward air trajectories on hazy days (a: summer; b: winter) and moderately hazy days (c: summer; d: winter) at Hong Kong during 2001–2004.

summertime SO_2 concentrations were similar to those in winter. The unique seasonal patterns in O_3 concentrations are due to the combined effects of the air mass origins and climatic characteristics associated with the monsoon systems affecting southeast China (Chan et al., 1998; Chan and Chan, 2000) – specifically, due to the continental outflow of aged air masses from the east Asian coast and the favourable meteorological conditions (bright sunshine, strong solar radiation, high temperatures and stable atmosphere), regional formation and accumulation of O_3 is enhanced in autumn (Chan et al., 1998; Chan and Chan, 2000). Unlike the seasonal cycles of PM_{10}, NO_2 and NO_x, there is no apparent significant seasonal cycle in SO_2 concentrations. The HKEPD (1997) suggested that this is probably due to increasing coal usage in power plants as a consequence of higher electricity demand for air conditioning purposes in summer in this subtropical region. Further detailed analysis is needed.

Ozone concentrations showed a substantial increase with a trend of 0.90 μg m^{-3} (≈ 0.45 ppbv) per yr, which agrees reasonably well with the findings of Chan et al. (2004), based on data from 1984 to 2004. O_3 concentrations decreased over the period 1984–1989 (-2.01 μg m^{-3} per yr, p < 0.01), while the increases mainly occurred from 1990 onwards (1.06 μg m^{-3} per yr, p < 0.001). This rate is very close to the background O_3 trend of south China from 1994–2007 (0.55 ppbv per yr) reported by Wang et al. (2009). The most pronounced annual increases in O_3 were observed in autumn (Table 1, Fig. 3), probably owing to increases in emissions of O_3 precursors in upwind source regions, i.e., the eastern coastal regions of China (Wang et al., 2009), supporting previous findings that overall O_3 increases were related to the regional increase in surface O_3 concentrations due to transport of precursors (which also display an increasing trend) from south China and east Asia (Chan et al., 2004; Wang et al., 2009). The onset of the

steepest increases in O_3 and RV both occurred in 1990, and the most pronounced trends in O_3 and RV both occurred in autumn. Such coincidence may point towards a relationship between O_3 concentration and RV, which is discussed in section 3.4.

Starting to increase from 1984, SO_2 concentrations reached a peak in 1993, after which they decreased slowly until 1999 when another upward trend started, peaking in 2008, after which a notable decreasing trend was observed. The increase rates during the periods of 1984–1993 and 1999–2008 were 0.88 and 0.67 $\mu g\ m^{-3}$ per yr, respectively ($p < 0.01$). The decreases from 1993 onwards were due to the effective bans of high-sulphur fuel usage and reduction of power plant emissions in the Hong Kong region (HKEPD, 1997), while the recent increase has been attributed (in part) to increases in SO_2 emissions in both Hong Kong and nearby Shenzhen (Chan and Yao, 2008) (Fig. 6). Other potential contributors to the recent SO_2 trend include ship emissions/bunker fuel usage: SO_2 emissions from shipping increased steadily from 1990 (Fig. 6), with some indications that this inventory may be underestimated as sulphur-rich bunker oils (containing up to ~5%

sulphur) would potentially be used by ocean going vessels outside local waters and such unregulated emissions are not included in the (national) inventory (Hong Kong Citizens Party, 2000). The total SO_2 emission inventory also neglects unrecorded imports of bunker fuel from mainland China to Hong Kong (Hong Kong Citizens Party, 2000). Regional emissions in east China are the other important factor affecting SO_2 concentration changes in southeast China (Lu et al., 2010). The notable decrease in SO_2 concentrations during the most recent years considered (2008–2010; Fig. 2) is coincident with decreases in SO_2 emissions following widespread and efficient implementation of Fuel Gas Desulfurization (FGD) devices in power plants during the 11th Five-Year Plan period (2006–2010) (Lu et al., 2010; Wan et al., 2011).

The PM_{10}, NO_x and NO_2 concentrations fluctuated within certain ranges (with annual means of 33–49 $\mu g\ m^{-3}$, 60–118 $\mu g\ m^{-3}$ and 30–67 $\mu g\ m^{-3}$ respectively) over the past 27 yr (not shown). According to the inventory of HKEPD (www.epd.gov.hk), emissions of these air pollutants in Hong Kong exhibited a decreasing trend from the 1990s (Fig. 6). If these inventory changes are correct,
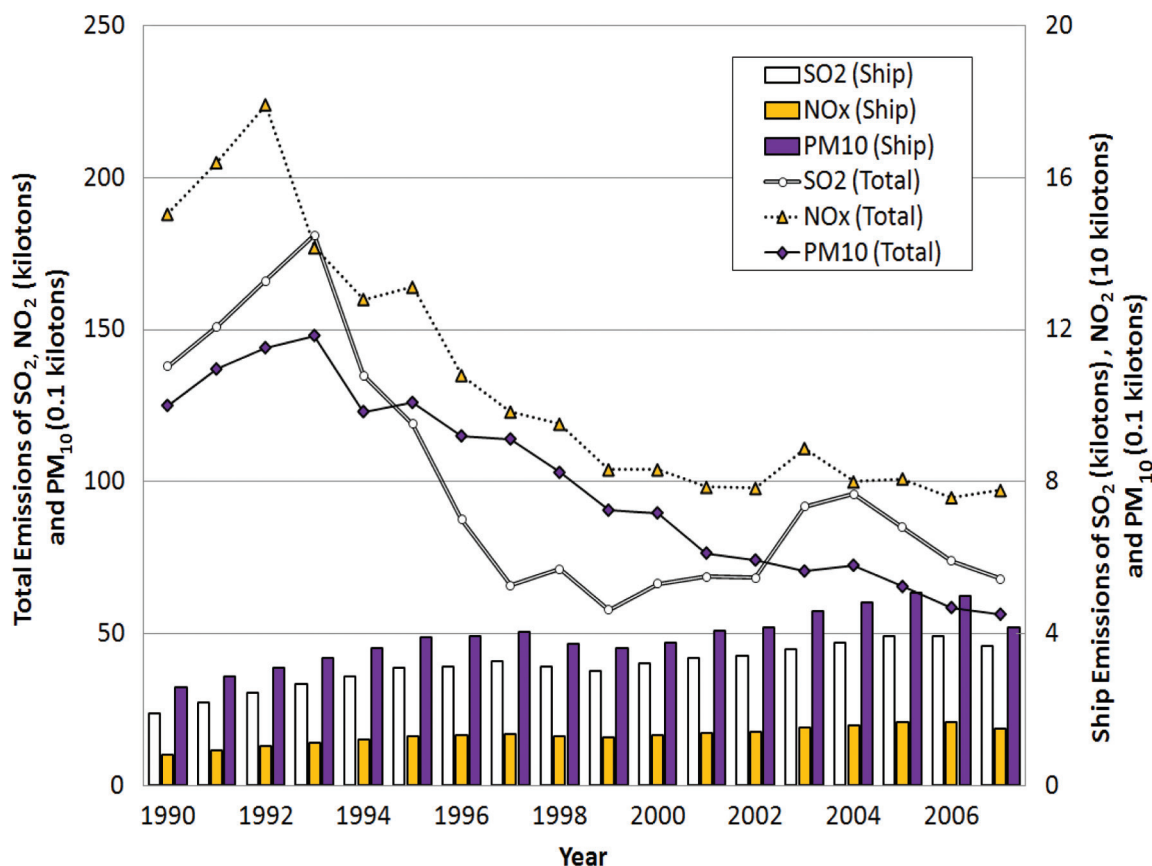

Fig. 6. Annual total emissions and ship emissions of SO_2, NO_x and PM_{10} (Data source: http://www.epd.gov.hk/epd/english/environmentinhk/air/data/emission_inve.html).

the observed pollutant levels highlight again the impact of pollutant emissions in upwind regions and transport on atmospheric composition in southeast China. Noticeably, positive trends of SO_2 and NO_2 were apparent in their autumn concentrations during 1984–2010 (Table 1). The SO_2 trend indicates a combined impact of long-range transport of polluted air masses, and regional emission in southeast China including Shenzhen and Hong Kong. The NO_2 trend may reflect increasing regional ozone levels enhancing NO-to-NO_2 conversion through the reaction $NO + O_3 \rightarrow NO_2 + O_2$ (Chan et al., 1998). Changes in CO and volatile organic compounds (VOCs) may also contribute to this trend through NO-peroxy radical reactions. Strong positive correlations between O_3 and CO concentrations were previously found in late spring to early autumn in this region (Chan et al., 2002), and O_3 formation in the Hong Kong region is VOC-limited (Huang et al., 2005). Oxidant analyses – O_x vs. NO_x regression (where O_x is the sum of the mixing ratios of NO_2 and O_3) (Clapp and Jankin, 2001) – indicated that local contribution to O_x kept decreasing before 1991, when all coal-fired power plants had installed low-NO_x burners. Overall, the coincident increases in O_3 and RV, and autumn increases in SO_2 and NO_2, point towards related causes, which are discussed in the following sections.

3.3. Relationship between visibility and air pollutants

Linear regression analyses were performed using multiple regression methods to examine the possible relationships between RV and air pollutants in Hong Kong (Table 2). Note that insignificant ($p > 0.05$) parameters are not shown in the regression model equations/coefficients listed in Table 2a; full values of the regression coefficient and partial correlation coefficients can be found in Table 2b. As PM_{10} monitoring started in 1993, the regression analyses including all five pollutant species (as independent variables) covers the period of 1993–2010 (model 1), while that for the whole period only includes four pollutant species (O_3, SO_2, NO_x, NO_2; model 2). In order to investigate the possible effects of in/exclusion of PM_{10} as an independent variable, we also repeated the analysis for 1993–2010 using O_3, SO_2, NO_x and NO_2 only (model 3).

A parallel analysis for the period 1984–1992 (model 4) was also performed for comparison between the former and latter periods. All regressions were examined by the f-test and the values given (Table 2a) were statistically significant ($p < 0.001$), meaning that RV was significantly correlated with levels of the various air pollutants.

In the model for the period 1984–2010 (model 2), the partial correlation coefficients between RV and O_3, SO_2 and NO_2 all passed the student t-test, i.e., during those 27 yr, of those factors considered, the visibility reduction was primarily influenced by O_3, SO_2 and NO_2. In the model for 1993–2010 (models 1 & 3), regardless of whether PM_{10} was included or not, the coefficients of partial correlation for O_3, SO_2, NO_2 passed the student t-test, while in that for 1984–1992 (model 4), only the coefficients of partial correlation for NO_2 and NO_x passed the student t-test. These results imply that there may have been changes in the dominant factors governing reductions in visibility, from influences of NO_2 and NO_x before 1993 to those of O_3, SO_2 and NO_2 afterwards.

3.4. Implications of visibility degradation and air quality changes

3.4.1. Formation of secondary sulphate in an O_3-enhanced atmosphere.
The accumulation of O_3 in the atmosphere increases the rate of production of several oxidants including OH and HO_2 radicals and H_2O_2, which have been found to play a significant role in secondary particle formation (Rae et al., 2007; Leibensperger et al., 2011). The simultaneous increases in O_3 concentration and RV, and their significant correlation identified here, imply that enhanced O_3 (and probably other oxidant) concentrations in southeast China may have a substantial impact on visibility degradation. Moreover, SO_2 levels were found to be significantly correlated with RV, but only after the 1990s, when both O_3 concentrations and RV increased notably. The difference in the regression/correlation results before and after 1993 suggests that the importance of O_3 and SO_2 in visibility impairment has increased over recent years. Under the condition of enhanced atmospheric oxidation capacity, SO_2 can be oxidized to secondary sulphate more rapidly (Unger et al., 2006), especially in the case that solar

Table 2a. Summary of equations calculated by multiple linear regression method

Regression model	Period	Independent variables	Equation[a]
Model 1	1993–2008	O_3, SO_2, NO_x, NO_2, PM_{10}	$[RV] = 0.17 [SO_2] + 0.31 [NO_2] + 0.17 [O_3] - 15.89$
Model 2	1984–2008	O_3, SO_2, NO_x, NO_2	$[RV] = 0.20 [SO_2] + 0.11 [NO_2] + 0.27 [O_3] - 12.63$
Model 3	1993–2008	O_3, SO_2, NO_x, NO_2	$[RV] = 0.18 [SO_2] + 0.32 [NO_2] + 0.18 [O_3] - 16.34$
Model 4	1984–1992	O_3, SO_2, NO_x, NO_2	$[RV] = 0.11 [NO_x] - 0.09 [NO_2] - 1.12$

[a]Units of RV are % and those of all air pollutants are $\mu g\ m^{-3}$.

Table 2b. Summary of regression coefficients and partial correlation coefficients calculated by the multiple linear regression method

Regression model	Period	Independent variables	Partial correlation coefficient	Regression coefficient ($\pm$ standard error)
Model 1	1993–2010	O_3	0.25	0.17 ± 0.05
		SO_2	0.16[a]	0.17 ± 0.08
		NO_x	0.01	0.00 ± 0.03
		NO_2	0.28[b]	0.31 ± 0.08
		PM_{10}	0.02	0.01 ± 0.06
Model 2	1984–2010	O_3	0.38[b]	0.27 ± 0.03
		SO_2	0.16[b]	0.20 ± 0.06
		NO_x	0.10	0.04 ± 0.02
		NO_2	0.17[c]	0.11 ± 0.04
Model 3	1993–2010	O_3	0.23[b]	0.18 ± 0.04
		SO_2	0.17[a]	0.18 ± 0.07
		NO_x	0.01	0.00 ± 0.03
		NO_2	0.40[b]	0.32 ± 0.05
Model 4	1984–1992	O_3	-0.09	-0.04 ± 0.04
		SO_2	0.13[a]	0.06 ± 0.05
		NO_x	0.43[b]	0.11 ± 0.02
		NO_2	-0.27[a]	-0.10 ± 0.03

[a]Significance level $p < 0.05$.
[b]Significance level $p < 0.001$.
[c]Significance level $p < 0.01$.

radiation was also slightly increasing (cloud cover decreasing) since the 1990's (www.hko.gov.hk). Chemical speciation of $PM_{2.5}$ in Hong Kong was intensively measured at an urban roadside station (Mong Kok) and two urban stations (Tsuen Wan and Yuen Long) during the (full) years of 2001, 2005 and 2009 (Chow et al., 2010). Combined with the ambient air quality data collected by the HKEPD, increasing ratios of sulphate concentration to concentrations of sulphate plus SO_2, $[SO_4^{2-}]/([SO_4^{2-}] + [SO_2])$, were found for all stations (Fig. 7), highlighting that secondary sulphate formation in $PM_{2.5}$ has increased over this period (although sulphate concentrations decreased slightly at the very end of the 25-yr period considered here, in 2009, which was owing to the nationwide implementation of FGD devices and the resulting decreases in SO_2 concentrations, as shown in Fig. 2). Wang (2003) found that sulphate, of which $\sim 96\%$ arose from regional formation, accounted for 33–51% of the total light extinction in Hong Kong, supporting the concept of an increasing role for O_3 (and its derived oxidants) in S(IV) to S(VI) processing, aerosol abundance and hence impact on visibility in southeast China. These data indicate that secondary sulphate is the predominant factor responsible for the visibility degradation apparent over the past two decades. The chemical mechanism of S(IV) to S(VI) transformation has been described extensively (e.g., Penkett et al., 1979; Stockwell and Calvert, 1983; Liang and Jacobson, 1999; Seinfeld and Pandis, 2006). The major pathways for atmospheric S(IV) oxidation are gas-phase oxidation of SO_2 by OH radical and aqueous oxidation of dissolved SO_2 with dissolved H_2O_2 or O_3.

The life time of SO_2 with respect to oxidation by OH is of the order of 13 d (298 K; $[OH] = 1 \times 10^6$ molecule cm^{-3}), so that increases in O_3 (and hence OH and H_2O_2) will increase condensed-phase SO_4^{2-} as experienced in Hong Kong (i.e., the transit time is sufficiently short that increases in reactant abundance will directly affect the extent of SO_2 oxidation during advection to the measurement site). This hypothesis agrees with the findings from a recent study, in which SO_4^{2-} concentrations in east Asia were found to increase at a greater rate than SO_2 emissions and SO_2 concentrations because 'east Asia is a less oxidant-limited area than other parts of the world' (Lu et al., 2010). In southeast China, gas-phase oxidation could be of particular importance in summer/autumn due to the strong solar radiation and high levels of O_3 and hence OH production (Hofzumahaus et al., 2009). As peroxide production would be enhanced by increasing HO_x levels (via $HO_2 + HO_2$ and other peroxy radical reactions), particularly in the context of near-constant NO_x as found here, the route of H_2O_2 oxidation would be important in this region as well. Regarding O_3 oxidation, because of its dependency on high pH values (Chameides, 1984; Calvert et al., 1985), it seems unlikely to be a dominant oxidation pathway of secondary sulphate in southeast China, which is affected by acidic precipitation (Larssen et al., 2006). However, we also note that Hong Kong is a coastal city often affected by sea-breezes, and hence a significant amount of secondary sulphate ($\sim 9\%$ of total global sulphate production) can actually be generated by the $S(IV) + O_3$ pathway on sea-salt aerosols (Alexander et al., 2005).

Our current data do not allow us to further investigate these formation pathways, but the enhanced formation of secondary sulphate has been already supported and ascertained by the observed relationships and chemical speciation data presented above (Fig. 7). It is worthwhile to mention that the SO_2 concentrations around 1993 were comparable to those of the recent 21st century, whereas the occurrence of RV at that time was substantially lower than current-day levels (Fig. 2). Considering the relatively low O_3 concentrations at that time, this elucidates why RV did not correlate with SO_2 and O_3 during 1984–1992 (because the oxidation reaction of S(IV) to S(VI) was limited), and further highlights the important role of high O_3 levels in enhancing the photochemical formation of secondary pollutants such as sulphate, which contribute significantly
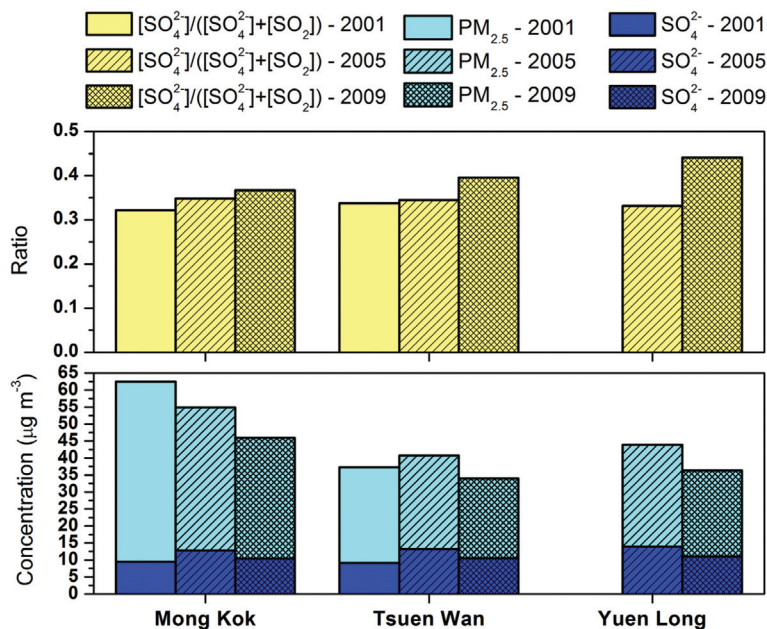
Fig. 7.   Ratios of sulphate concentrations in $PM_{2.5}$ to the concentrations of sulphate plus SO_2 (upper panel). $PM_{2.5}$ and sulphate concentration data (lower panel) were adopted from Chow et al. (2010).

to visibility reduction (Shao et al., 2006). Note that SO_2 emission in east China also kept increasing from 1985 to 2006 (Streets et al., 2000; Lu et al., 2010), suggesting that the visibility degradation in southeast China may in part be due to transport of secondary sulphate formed upwind (i.e., over the east China coast). Measurements of the mass-independent fractionated oxygen isotopes in sulphate allow the primary and secondary sulphate contributions to be identified, and the oxidation pathways of secondary sulphate to be quantified (Lee and Thiemens, 2001; Lee et al., 2001; Alexander et al., 2005; Patris et al., 2007; Dominguez et al., 2008). Such measurements can bring us closer to identifying the dominant oxidation mechanisms in the future.

3.4.2. Chemical coupling of O_3, NO_2 and other species. NO_2 contributes directly to visibility degradation due to its strong absorption in the blue region of the spectrum, which could partly explain its statistically significant correlation with RV occurrence, although it has previously been shown to account for only 2–5% of total light extinction in Hong Kong (Wang, 2003). Under high oxidant/ O_3/OH conditions, if CO or VOCs are present in sufficient amounts, the photostationary steady state of the NO-NO_2-O_3 cycle will be modified as NO_2 can be regenerated through the reaction between NO and HO_2 (or RO_2), resulting in net formation of O_3. As discussed above, the accumulation of O_3 in the atmosphere would amplify the production of several oxidants, and therefore the increase

in ambient NO_2 concentrations also indicates the impact of other secondary pollutants (O_3). The statistically significant correlations between RV occurrence and NO_2 concentrations thus further highlight the important role of secondary pollutants in visibility reduction in southeast China. Moreover, NO_2 could react with these oxidants to produce nitric acid (HNO_3) and peroxyacetyl nitrate (PAN). In the presence of NH_3, subsequent formation of particulate ammonium nitrate (NH_4NO_3) (Meng et al., 1997), one of the components of particulate matter identified as contributing to degrading visibility in the Hong Kong region (Lai and Sequeira, 2001; Cheung et al., 2005). However, the contribution of nitrate to total light extinction in this region has been found to be relatively small (4–5%) when compared with other species (Wang, 2003). The origin of the negative correlation between RV and NO_2 in Hong Kong during 1984–1992 is unclear, although the correlation is only significant to a lower confidence level than (for example) O_3. Besides sulphate and nitrate, secondary formation of other particulate species such as secondary organic aerosol (SOA) was also important. For instance, formation of dicarboxylic acids via photo-oxidation was recently observed in the PRD (Ho et al., 2011), which play an important role in affecting visibility and global radiative balance (Kawamura and Kaplan, 1987; Facchini et al., 1999); particulate organic matter has been found to be a major light scattering component in this region (Cheung et al., 2005) and contained a significant amount of secondary organic carbon in this region

(Cao et al., 2004). Wang (2003) suggested that organic carbon contributed 17–21% of the total light extinction in Hong Kong.

3.4.3. Other possible causes of visibility degradation.

We did not find a statistically significant correlation between RV and PM_{10} concentrations in this study, although visibility impairment is generally proportional to the loading of airborne particulate matter (PM), especially fine particles (e.g., $PM_{2.5}$), while Ho et al. (2003) found that 53–78% of the PM_{10} mass was made up of $PM_{2.5}$ in this region. The absence of significant correlation between PM_{10} and RV occurrence suggests that PM_{10} as a measure was not necessarily correlated with the concentrations of specific light scatterers/absorbers present, due to the variation in chemical speciation within aerosol particles. A more detailed long-term assessment of aerosol composition is required to give further insight into this variability. We also note that the PM_{10} concentrations in Hong Kong did not show a significant trend during the past 18 yr (1993–2010), when visibility continued to degrade steadily. Given that light is most effectively scattered by fine particles rather than coarse particles, this suggests that the loading of fine particles was increasing during recent years, resulting in the increase in occurrences of RV, while a decrease in coarse particle mass may have offset the (absolute) increase in fine particles, thus leading to relatively steady PM_{10} concentrations throughout the study period. According to the limited $PM_{2.5}$ samples collected from an urban station (Tsuen Wan) and a rural station (Tap Mun) in Hong Kong, the mass

concentrations of $PM_{2.5}$ did show increasing trends from 1999 to 2008 (HKEPD, 2009).

Some primary particles can also affect visibility, and variation in their emissions/abundance should not be neglected. For instance, elemental carbon (EC) is an effective light absorber (accounting for ∼20% of visibility reduction) and is the primary cause of visibility reduction in Guangzhou (Deng et al., 2008). In Hong Kong, although the EC levels are lower than those in Guangzhou (Cao et al., 2003; 2004), it was still found to contribute 12–26% to the total light extinction (Wang, 2003). Water-soluble potassium (K^+) has also been found to be associated with visibility degradation through light scattering in Hong Kong (Sequeira and Lai, 1998; Lai and Sequeira, 2001), probably indicating the contribution of biomass burning emissions, usually associated with the emission of multiple species with significant hygroscopic growth and light extinction capacity such as humic-like substances (Lin et al., 2010b). Visibility degradation in southeast China might therefore also be partly attributed to (trends in) biomass burning emissions, known to be an important air pollutant source in this region (Lin et al., 2010b; Sang et al., 2011). Finally, primary sulphate emissions from ships in this region may contribute to visibility degradation. Recent observations in California found that ship emissions contributed a high proportion (10–44%) of the non-sea-salt sulphate in fine PM (Dominguez et al. 2008), significantly higher than previous estimates (∼2–7%, e.g., Seinfeld and Pandis, 2006). Having a major international harbour, the Hong Kong region is strongly affected by ship emissions
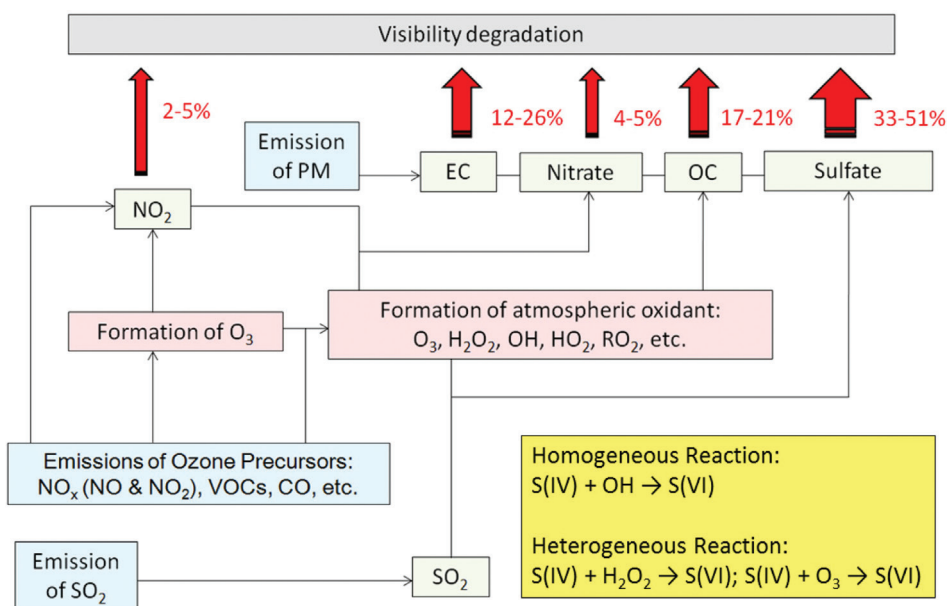

Fig. 8.   Chemical coupling among trace gases leading to impacts on visibility degradation in the Hong Kong region – see text for details. Percentage values indicate the light extinction contributions of various species given by Wang (2003).

(Corbett et al., 2007), with high loadings of EC, SO_2 and NO_y, attributed to ship activities at the port (Wang et al., 2003; Yu et al., 2004). Although long-term data of sulphate emissions from ships are not available, the steady increase in ship-emitted SO_2 (Fig. 6) recorded by the HKEPD may also contribute to the sulphate aerosol-driven increasing occurrence of RV. In summary, the chemical coupling among trace gases and impacts of atmospheric particulates on visibility degradation mentioned above are illustrated schematically in Fig. 8.

4. Summary

In this paper, we report measurements which show that atmospheric visibility in Hong Kong deteriorated rapidly in the last four decades, especially during the 1990s and beyond. Alongside visibility degradation, significant increases in concentrations of O_3 were observed from 1984 to 2010, while SO_2 concentrations increased through the periods from 1984 to 1993 and 1999 to 2010. The most pronounced increases in the occurrence of RV, and in O_3, SO_2 and NO_2 concentrations, were all observed in autumn. These results are attributed to the influence of rapid development and associated emissions in the highly populated cities in eastern China on atmospheric composition and hence visibility in downwind southeast China. As autumn is the season most favourable for the regional formation and accumulation of surface O_3 in the region, the trends identified here highlight the enhancement of regional surface O_3 and its effect on relevant oxidants and associated regional atmospheric oxidation chemistry enhancement. The RV was found to correlate significantly with NO_2 and NO_x in the 1980s, and with NO_2, SO_2 and O_3 from the 1990s onwards, suggesting that there have been changes in the major factors responsible for visibility degradation in Hong Kong. Several possible causes of visibility degradation are proposed; in particular the enhanced oxidation capacity may play a dominant role in increasing the formation of secondary particulates, especially secondary sulphate, which was supported by direct observations of sulphate concentrations in $PM_{2.5}$ in previous research. The enhancement of secondary particulate formation may modify both loadings and composition of tropospheric aerosol, and thus have vital impacts on regional climate via aerosol radiative forcing, in addition to the immediately apparent environmental impact of reduced visibility. Further investigation into the inter-annual variation of secondary pollutant levels is needed in the future to better understand changes in atmospheric oxidation capacity and their impact on atmospheric composition. Occurrence of RV was not correlated with PM_{10} levels, suggesting that fine particulate abundance varied at this location, while PM_{10} did not. This further suggests that PM_{10} mass concentra-

tions are not necessarily proportional to visibility, and that policy measures which focus upon PM_{10} reductions as air quality metrics may not achieve corresponding improvements in visibility.

5. Acknowledgements

References

Alexander, B., Park, R. J., Jacob, D. J., Li, Q. B., Yantosca, R. M. and co-authors. 2005. Sulphate formation in sea-salt aerosols: constraints from oxygen isotopes. *J. Geophys. Res.* **110**, D10307, 12. DOI: 10.1029/2004JD005659.

Calvert, J. G., Lazarus, A., Kok, G. L., Heikes, B. G., Walega, J. G. and co-authors. 1985. Chemical mechanism of acid generation in the troposphere, *Nature* **317**, 27–35.

Cao, J. J., Lee, S. C., Ho, K. F., Zhang, X. Y., Zou, S. C. and co-authors. 2003. Characteristics of carbonaceous aerosol in Pearl River Delta Region, China during 2001 winter period. *Atmos. Environ.* **37**, 1451–1460.

Cao, J. J., Lee, S. C., Ho, K. F., Zou, S. C., Fung, K. and co-authors. 2004. Spatial and seasonal variations of atmospheric organic carbon and element carbon in Pearl River Delta Region, China. *Atmos. Environ.* **38**, 4447–4456.

Chameides, W. L. 1984. The photochemistry of remote marine stratiform cloud. *J. Geophys. Res.* **89**(D3), 4739–4755.

Chan, L. Y., Chan, C. Y. and Qin, Y. 1998. Surface ozone pattern in Hong Kong. *J. Appl. Meteorol.* **31**, 159–268.

Chan, C. Y. and Chan, L. Y. 2000. Effect of meteorology and air pollutant transport on ozone episodes at a subtropical coastal Asian city, Hong Kong. *J. Geophys. Res.* **105**(D16), 20707–20724.

Chan, C. Y., Chan, L. Y., Lam, K. S., Li, Y. S., Harris, J. M. and co-authors. 2002. Effect of Asian air pollution transport and photochemistry on carbon monoxide variability and ozone production in subtropical coastal south China. *J. Geophys. Res.* **107**(D24), 4746. DOI: 10.1029/2002JD002131.

Chan, C. Y., Chan, L. Y. and Harris, J. M. 2004. Urban and background ozone trend in 1984–1999 at subtropical Hong Kong South China. *Ozone-Sci. Eng.* **25**, 513–522.

Chan, C. K. and Yao, X. H. 2008. Air pollution in mega cities in China. *Atmos. Environ.* **42**, 1–42.

Che, H. Z., Zhang, X. Y., Li, Y., Zou, Z. J. and Qu, J. J. 2007. Horizontal visibility trends in China 1981–2005. *Geophys. Res. Lett.* **34**, L24706, 5. DOI: 10.1029/2007GL031450.

Che, H. Z., Zhang, X. Y., Li, Y., Zou, Z. J., Qu, J. J. and Hao, X. J. 2009. Haze trends over the capital cities of 31 provinces in China, 1981–2005. *Theor. Appl. Climatol.* **97**(3–4), 235–242.

Cheung, H. C., Wang, T., Baumann, K. and Guo, H. 2005. Influence of regional pollution outflow on the concentrations of fine particulate matter and visibility in the coastal area of southern China. *Atmos. Environ.* **39**, 6463–6474.

Chow, J. C., Watson, J. G., Kohl, S. D. and Chen, L.-W. A. 2010. *Measurements and validation for the 2008/2009 particulate matter study in Hong Kong*. Reno, USA: Desert Research Institute. NV.

Clapp, L. J. and Jenkin, M. E. 2001. Analysis of the relationship between ambient levels of O_3, NO_2 and NO as a function of NO_x in the UK. *Atmos. Environ.* **35**, 6391–6405.

Deng, X. J., Tie, X. X., Wu, D., Zhou, X. J., Bi, X. Y. and co-authors. 2008. Long-term trend of visibility and its characterizations in the Pearl River Delta (PRD) region, China, *Atmos. Environ.* **42**(7), 1424–1435.

Dominguez, G., Jackson, T., Brothers, L., Barnett, B., Nguyen, B. and co-authors. 2008. Discovery and measurement of an isotopically distinct source of sulphate in Earth's atmosphere. *Proc. Natl. Acad. Sci.* **105**(35), 12769–12773.

Draxler, R. R. and Rolph, G. D. 2010. *HYSPLIT (Hybrid Single-Particle Lagrangian Integrated Trajectory) Model*. NOAA Air Resources Laboratory, Silver Spring, MD. Online at: http://ready.arl.noaa.gov/HYSPLIT.php

Facchini, M. C., Mircea, M., Fuzzi, S. and Charlson, R. J. 1999. Cloud albedo enhancement by surface-active organic solutes in growing droplets. *Nature* **410**, 257–259.

Ho, K. F., Lee, S. C., Chan, C. K., Yu, J. C., Chow, J. C. and Yao, X. H. 2003. Characterization of chemical species in $PM_{2.5}$ and PM_{10} aerosols in Hong Kong. *Atmos. Environ.* **37**, 31–39.

Ho, K. F., Ho, S. S. H., Lee, S. C., Kawamura, K., Zou, S. C. and co-authors. 2011. Summer and winter variations of dicarboxylic acids, fatty acids and benzoic acid in $PM_{2.5}$ in the Pearl River Delta Region, China. *Atmos. Chem. Phys.* **11**, 2197–2208.

Hofzumahaus, A., Rohrer, F., Lu, K., Bohn, B., Brauers, T. and co-authors. 2009. Amplified trace gas removal in the troposphere. *Science* **324**, 1702–1704.

Hong Kong Citizens Party. 2000. *Clearing the air – still a long way to go: a comprehensive review of air pollution problems and solutions*. Hong Kong: Citizens Party. Paper No. CB(2)2460/99-00(01). Online at: http://www.legco.gov.hk/yr99-00/english/panels/tp/papers/2460e01.pdf

Hong Kong Environmental Protection Department. 1997. *Air Quality in Hong Kong 1996*. Report No. EPD/TR6/97. Hong Kong: The Government of the Hong Kong Special Administrative Region. Online at: http://www.epd-asg.gov.hk/english/report/files/aqr96e.pdf

Hong Kong Environmental Protection Department. 2009. *Review of Air Quality Objectives and Development of a Long Term*

Air Quality Strategy for Hong Kong – Feasibility Study. Hong Kong: Ove Arup & Partners Hong Kong. Online at: http://www.epd.gov.hk/epd/english/environmentinhk/air/studyrpts/files/Final_Report_091013.pdf

Hong Kong Environmental Protection Department. 2010. *Air Quality in Hong Kong 2009*. Report No. EPD/TR01/10. Hong Kong: The Government of the Hong Kong Special Administrative Region. Online at: http://www.epd-asg.gov.hk/english/report/files/aqr09e.pdf

Huang, J. P., Fung, J. C. H., Lau, A. K. H. and Qin, Y. 2005. Numerical simulation and process analysis of typhone-related ozone episodes in Hong Kong. *J. Geophys. Res.* **110**, D05301. 17. DOI: 10.1029/2004JD004914.

Huang, W., Tan, J., Kan, H., Zhao, N., Song, W. and co-authors. 2009. Visibility, air quality and daily mortality in Shanghai, China. *Sci. of the Total Environ.* **407**, 3295–3300.

Kawamura, K. and Kaplan, I. R. 1987. Motor exhaust emissions as a primary source for dicarboxylic acids in Los Angeles ambient air. *Environ. Sci. Technol.* **21**(1), 105–110.

Kim, K. W., Kim, Y. J. and Oh, S. J. 2001. Visibility impairment during Yellow Sand periods in the urban atmosphere of Kwangju, Korea. *Atmos. Environ.* **35**, 5157–5167.

Lai, L. Y. and Sequeira, R. 2001. Visibility degradation across Hong Kong: its components and their relative contributions. *Atmos. Environ.* **35**, 5861–5872.

Lam, K. S., Wang, T. J., Chan, L. Y., Wang, T. and Harris, J. 2001. Flow patterns influencing the seasonal behavior of surface ozone and carbon monoxide at a coastal site near Hong Kong. *Atmos. Environ.* **35**, 3121–3135.

Larssen, T., Lydersen, E., Tang, D., He, Y., Gao, J. and co-authors. 2006. Acid rain in China. *Environ. Sci. Technol.* **40**(2), 418–425.

Lee, C. C. W. and Thiemens, M. H. 2001. Mass independent oxygen isotopic composition of atmospheric sulphate from a coastal and high alpine region: a mass-independent anomaly. *J. Geophys. Res.* **105**(D15), 17359–17373.

Lee, C. C. W., Savarino, J. and Thiemens, M. H. 2001. Mass independent oxygen isotopic composition of atmospheric sulphate: origin and implication for the present and past atmosphere of Earth and Mars. *Geophys. Res. Lett.* **28**(9), 1783–1786.

Lee, Y. L. and Sequeira, R. 2002. Water-soluble aerosol and visibility degradation in Hong Kong during autumn and early winter, 1998. *Environ. Pollut.* **116**, 225–233.

Leibensperger, E. M., Mickley, L. J., Jacob, D. J. and Barrett, S. R. H. 2011. Intercontinental influence of NO_x and CO emissions on particulate matter air quality. *Atmos. Environ.* **45**, 3318–3324.

Leung, Y. K., Cheng, Y. Y. and Wu, M. C. 2004. *Long-term change of atmospheric visibility in Hong Kong*. Reprint No. 565. Hong Kong: Hong Kong Observatory (in Chinese).

Liang, J. Y. and Jacobson, M. Z. 2000. Effects of subgrid segregation on ozone production efficiency in a chemical model. *Atmos. Environ.* **34**(18), 2975–2982.

Lin, J., Nielsen, C.P., Zhao, Y., Lei, Y., Liu, Y. and co-authors. 2010a. Recent changes in particulate air pollution over China observed from space and the ground: effectiveness of emission control. *Environ. Sci. Technol.* **44**, 7771–7776.

Lin, P., Engling, G. and Yu, J. Z. 2010b. Humic-like substances in fresh emissions of rice straw burning and in ambient aerosols in the Pearl River Delta Region, China. *Atmos. Chem. Phys.* **10**, 6487–6500.

Liu, B., Xu, M. and Henderson, M. 2010. Where have all the showers gone? Regional declines in light precipitation evens in China, 1960–2000. *Int. J. Climatol.* **31**(8), 1177–1191. DOI: 10.1002/joc.2144.

Lu, Z., Streets, D. G., Zhang, Q., Wang, S., Carmichael, G. R. and co-authors. 2010. Sulphur dioxide emission in China and sulphur trends in east Asia since 2000. *Atmos. Chem. Phys.* **10**, 6311–6331.

Meng, Z. 1997. Chemical coupling between atmospheric ozone and particulate matter. *Science* **277**(5322), 116–119.

Patris, N., Cliff, S. S., Quinn, P. K., Kasem, M. and Thiemens, M. H. 2007. Isotopic analysis of aerosol sulphate and nitrate during ITCT-2k2: determination of different formation pathways as a function of particle size. *J. Geophys. Res.* **112**, D23301, 17. DOI: 10.1029/2005JD006214.

Penkett, S. A., Jones, B. M. R. and Eggleton, A. E. J. 1979. A study of SO_2 oxidation in stored rainwater samples, Atmos. *Environ.* **13**(1), 139–147.

Rae, J. G. L., Johnson, C. E., Bellouin, N., Boucher, O., Haywood, J. M. and co-authors. 2007. Sensitivity of global sulphate aerosol production to changes in oxidant concentrations and climate. *J. Geophys. Res.* **112**, D10312, 10. DOI: 10.1029/2006JD007826.

Richter, A., Burrows, J. P., Nüß, H., Granier, C. and Niemeier, U. 2005. Increase in tropospheric nitrogen dioxide over China observed from space. *Nature* **437**, 129–132.

Rolph, G. D. 2010. *Real-time Environmental Applications and Display sYstem (READY)*. NOAA Air Resources Laboratory, Silver Spring, MD. Online at: http://ready.arl.noaa.gov

Rosenfeld, D., Dai, J., Yu, X., Yao, Z., Xu, X. and co-authors. 2007. Inverse relations between amounts of air pollution and orographic precipitation. *Science* **315**, 1396–1398.

Sang, X. F., Chan, C. Y., Engling, G., Chan, L. Y., Wang, X. M. and co-authors. 2011. Levoglucosan enhancement in ambient aerosol during springtime transport events of biomass burning smoke to southeast China. *Tellus B* **63B**, 129–139.

Seinfeld, J. H. and Pandis, S. N. 2006. *Atmospheric Chemistry and Physics*. New York: Wiley-Interscience.

Sequeria, R. and Lai, K. H. 1998. The effect of meteorological parameters and aerosol constituents on visibility in urban Hong Kong. *Atmos. Environ.* **32**, 2865–2871.

Sequeira, R. and Lai, K.-H. 1998. The effect of meteorological parameters and aerosol constituents on visibility in urban Hong Kong. *Atmos. Environ.* **32**(16), 2865–2871.

Shao, M., Tang, X. Y., Zhang, Y. H. and Li, W. J. 2006. City clusters in China: air and surface water pollution. *Front. Ecol. Environ.* **4**(7), 353–361.

Stockwell, W. R. and Calvert, J. G. 1983. The mechanism of the $HO-SO_2$ reaction. *Atmos. Environ.* **17**(11), 2231–2235.

Street, D. G., Tsai, N. Y., Akimoto, H. and Oka, K. 2000. Sulphur dioxide emissions in Asia in the period 1985–1997. *Atmos. Environ.* **34**(26), 4413–4424.

Thach, T. Q., Wong, C. M., Chan, K. P., Chau, Y. W., Chung, Y. N. and co-authors. 2010. Daily visibility and mortality: assessment of health benefits from improved visibility in Hong Kong. *Environ Res.* **110**(6), 617–623. DOI: 10.1016/j.envres.2010.05.005.

Tsai, Y. I. 2005. Atmospheric visibility trends in an urban area in Taiwan 1961–2003. *Atmos. Environ.* **39**, 5555–5567.

Unger, N., Shindell, D. T., Koch, D. M. and Streets, D. G. 2006. Cross influences of ozone and sulphate precursor emissions changes on air quality and climate. *Proc. Natl. Acad. Sci.* **103**(12), 4377–4380.

Wan, J. M., Lin, M., Chan, C. Y., Zhang, Z. S., Engling, G. and co-authors. 2011. Change of air quality and its impact on atmospheric visibility in central-western Pearl River Delta. *Environ. Monit. Assess.* **110**(6), 617–623. DOI: 10.1007/s10661-010-1338-2.

Wang, T. 2003. *Study of Visibility Reduction and its Causes in Hong Kong*. Hong Kong: The Hong Kong Polytechnic University.

Wang, T., Wei, X. L., Ding, A. J., Poon, C. N., Lam, K. S. and co-authors. 2009. Increasing surface ozone concentrations in the background atmosphere of southern China, 1994–2007. *Atmos. Chem. Phys.* **9**, 6217–6227.

Yeung, K. K., Chang, W. L., Wan, B., Kimura, F. and Yoshikawa, T. 1990. Simulation of boundary layer flow in Hong Kong. *Atmos. Environ.* **25A**, 2161–2172.

Yu, J. Z., Tung, J. W. T., Wu, A. W. M., Lau, A. K. H., Louie, P. K. K. and co-authors. 2004. Abundance and seasonal characteristics of elemental and organic carbon in Hong Kong PM_{10}. *Atmos. Environ.* **38**(10), 1511–1521.

Zhang, Y. N., Zhang, Z. S., Chan, C. Y., Engling, G., Sang, X. F. and co-authors. 2011. Levoglucosan and carbonaceous species in the background aerosol of coastal southeast China: case study on transport of biomass burning smoke from the Philippines. *Environ. Sci. Pollut. Res.* DOI: 10.1007/s11356-011-0548-7.

Zhang, Z. S., Engling, G., Lin, C. Y., Chou, C. C. K., Lung, S. C. C. and co-authors. 2010. Chemical speciation, transport and contribution of biomass burning smoke to ambient aerosol in Guangzhou, a mega city of China. *Atmos. Environ.* **44**, 3187–3195.